The Abdus Salam International Centre for Theoretical Physics

United Nations Educational, Scientific and Cultural Organization

IAEA International Atomic Energy Agency

1965-8

9th Workshop on Three-Dimensional Modelling of Seismic Waves Generation, Propagation and their Inversion

22 September - 4 October, 2008

Structure and rheology of lithosphere in Italy and surrounding

G.F. Panza
Dept. of Earth Sciences/ICTP, Trieste

panza@dst.units.it

doi: 10.1111/j.1365-3121.2008.00805.x

Structure and rheology of lithosphere in Italy and surrounding

G. F. Panza[1,2] and R. B. Raykova[3,4]

[1]*Department of Earth Sciences, University of Trieste, Via E. Weiss 4, I-34127 Trieste, Italy;* [2]*International Centre for Theoretical Physics, ESP/SAND section, Strada Costiera 11, I-34014 Trieste, Italy;* [3]*Geophysical Institute of Bulgarian Academy of Sciences, Acad. G. Bonchev str. blok 3, 1113 Sofia, Bulgaria;* [4]*Istituto Nazionale di Geofisica e Vulcanologia – Sezione di Bologna, Via D. Creti 12, I-40128 Bologna, Italy*

ABSTRACT

We define the structure and rheology of the lithosphere in Italy and surrounding, combining the cellular velocity models derived from nonlinear tomographic inversion with the distribution vs. depth of hypocentres to assess the brittle properties of the Earth's crust. We average, over cells sized 1×1 degree, the mechanical properties of the uppermost 60 km of the Earth, along with seismicity, grouping hypocentral depths in 4-km intervals. For most of the cells, the earthquake energy is concentrated in the upper crust (4–12 km). For some regions, where orogenic processes occur, the release of earthquake energy is shallower and limited to the uppermost 10 km of the crust. Ambiguities in the structural models are minimized considering the hypocentral distribution, mainly to define the location of the Moho boundary, when its identification, based on shear-wave velocities, is not straightforward.

Terra Nova, 20, 194–199, 2008

Introduction

Anderson (2007) gives a good and long-overdue contribution that properly emphasizes the limits of currently available, and widely used, tomographic maps. In addition to the cases discussed by Anderson (2007), a large plume has been proposed to be present beneath the Western Atlantic and Central Europe (Hoernle *et al.*, 1995), even though, because of the resolution (~0.4% variation in V_p), its deeper part (below ~300 km) is barely distinguishable, if not indistinguishable from normal mantle.

The Western Mediterranean represents a key place where geophysical and geochemical data can be combined to test the relationships between magmatism and mantle structure, and to place constraints on the roles of shallow-mantle vs. deep plumes in the genesis of the magmatism and the geodynamic evolution of the area (Panza *et al.*, 2007a). Cadoux *et al.* (2007) suggest a possible lower mantle source for Italian volcanism, but our recently published *S*-wave tomography (*Panza et al.*, 2007b) indicates a shallow upper-mantle source for the Apennines-Tyrrhenian igneous system and the absence of a plume beneath Italy and the back-arc basin. In two non-colour-saturated cross-sections, in which geological and geophysical data of the TRANSMED Project (Carminati *et al.*, 2004) are tied to the shear-wave tomography models, there is no evidence of a deeply rooted plume beneath the back-arc basin: along W-directed subduction zones the retreat of the slab requires that the upper mantle fills in the space left by the removed lithosphere (Doglioni, 1991; Doglioni *et al.*, 1999a,b).

The presence of a plume beneath Italy would be expected to be recorded in elevated heat flow and the consequently attenuated brittle behaviour of the lithosphere, i.e. lower level of seismic energy release. We investigated this by studying the structure and rheology of the lithosphere. We combined the cellular model derived from the nonlinear tomographic inversion by Farina (2006) and Panza *et al.* (2007a), with the distribution vs. depth of earthquakes, to assess the brittle properties of the fragile Earth, and we have given a synoptic representation of the mechanical properties of the uppermost 60 km, along with the seismicity, averaged over cells 1×1 degree in size. It is evident from the results that the model of a mantle plume beneath Italy should be discarded, supporting the voluminous petrological arguments against a plume that have already been reported (Peccerillo, 2005).

Correspondence: G. F. Panza, Department of Earth Sciences, University of Trieste, Via E. Weiss 4, I-34127 Trieste, Italy. Tel.: +39 040 5582117; fax: +39 040 5582111; e-mail: panza@units.it

Method

Figures 1–3 show a synoptic representation of the mechanical properties of the uppermost 60 km of the Earth. The cellular velocity models are presented in the leftmost graph for each cell and they are obtained by the nonlinear inversion of Rayleigh surface-wave dispersion data in the period range 5–150 s for group velocity, and 15–150 s for phase velocity (Panza and Pontevivo, 2004; Farina, 2006; Panza *et al.*, 2007a). The local dispersion data obtained by 2D tomography (Yanovskaya and Ditmar, 1990; Yanovskaya, 1997) are inverted by the nonlinear 'hedgehog' method (Panza, 1981). The *V*s models and their uncertainties are computed for each cell defined in the study region. Because of the well-known non-uniqueness of the inverse problem, for each cell, a set of models fit the dispersion data, all with similar levels of reliability. An optimized smoothing method called LSO (Panza *et al.*, 2007a; Boyadzhiev *et al.*, 2008) that fixes the cellular model as the one that has minimal divergence in velocity between neighbouring cells is used to define the representative cellular model by a formalized criterion.

The uppermost 60 km of the models obtained is shown in Figs 1–3: *V*s is colour coded for easier visualization of the velocity structure, the range of variability of the depth of the interfaces (the boundaries between layers can well be transition zones in their own right) and of the velocity is given for most of the parameterized layers (some values are omitted for graphical reasons). The red dots in the velocity models represent hypocentres; some

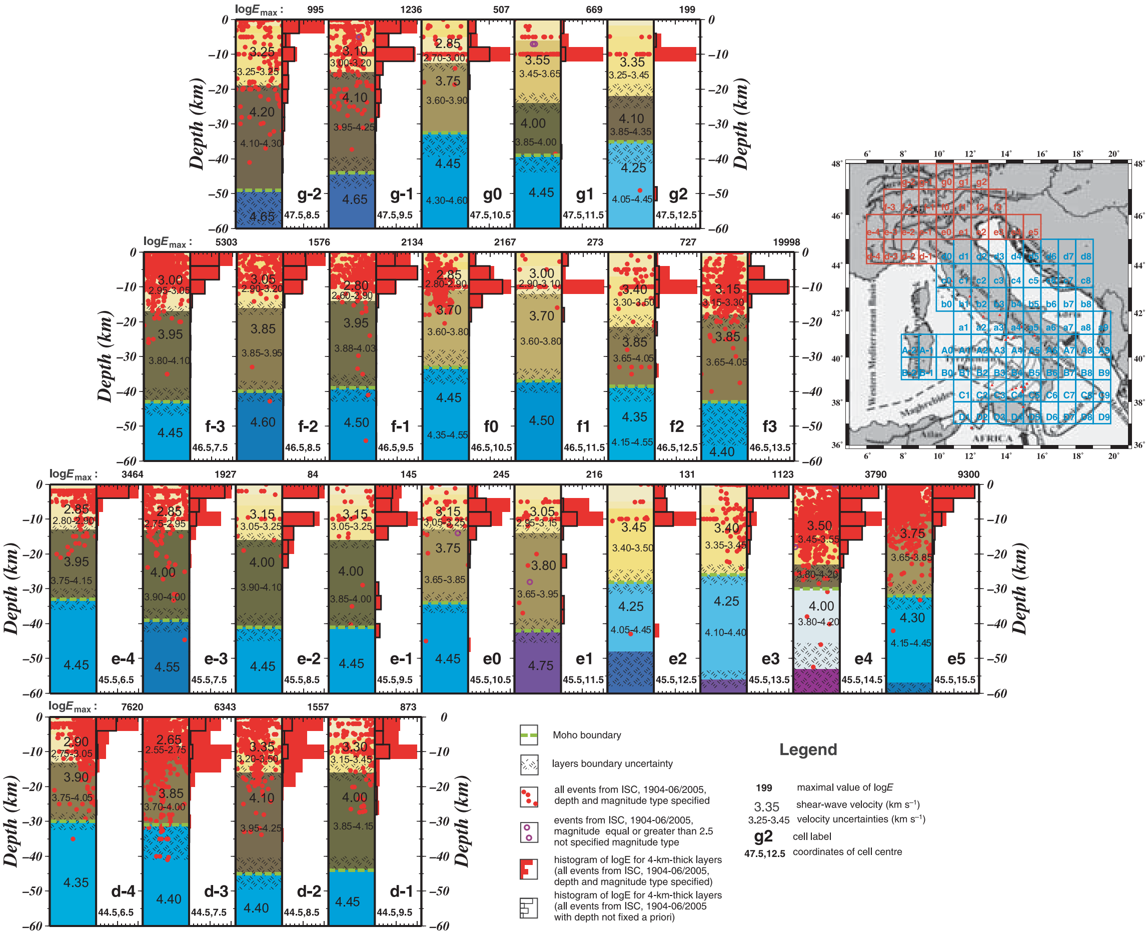

Fig. 1 The cellular Vs structures and related log$E$–h distribution of earthquakes, obtained grouping hypocentres in 4-km intervals, in North Italy and surrounding areas. The upper 60 km of the Earth model are plotted on the leftmost graph for each cell. The average Vs and its range of variability in km s^{-1} are printed on each layer and a hatched rectangular zone outlines the range of variability of their thicknesses. For the sake of clarity, in the uppermost crustal layers the values of Vs are omitted; these values are given in Farina (2006) and Panza *et al.* (2007b). The hypocentres with depth and magnitude type specified are denoted by red dots. The hypocentres with magnitude equal to or greater than 2.5, but of unspecified magnitude type, are denoted by purple circles. The normalized logarithm of seismic energy with respect to depth obtained by grouping hypocentres in 4-km intervals, is shown in the right hand graph for each cell. The filled red bars histogram represents the energy of all earthquakes from the revised ISC (2007) catalogue for 1904–June 2005. The black line histogram represents the energy of earthquakes for which the hypocentre depth is not fixed a priori in the ISC catalogue. At the bottom of this graph the cell label and the coordinates of the cell's center are given. The normalizing value of the maximum of the energy's logarithm logE_{max} is given on the horizontal axis of the energy-depth distribution graph. The location of each cell is shown in the map and superimposed on the structural and kinematic sketch of Italy and surrounding areas from Meletti *et al.* (2000). The red colour marks the cells that are presented in this figure and the blue colour marks all other cells studied in the paper.

earthquakes with unspecified kind of magnitude are plotted as purple circles.

We used the revised ISC (2007) catalogue for the period 1904–June 2005 and, using the relation of Richter (1958) $\log E = 1.5M_s + 11.4$, for each cell we computed the total energy released by the earthquakes, grouping hypocentres in 4-km intervals. The value of M_s is either directly taken from the ISC catalogue or computed from currently available relationships between M_s and other magnitudes (Peishan and Haitong, 1989). As the hypocentral depths did not exceed 60 km there was no need to correct M_s for the focal depth (Herak *et al.*, 2001). The energy of the earthquakes, for which only M_d is known, is calculated as follows. The regression relation constructed for the study region from the earthquakes for which M_d and M_l are known, is used to determine M_l which is then converted to M_s. The relationship obtained $M_l = 1.12M_d - 0.76$ is in agreement with similar relationship computed by Gasperini (2002) for the Italian region. The earthquake

 Terra Nova, Vol **20**, No. 3, 194–199

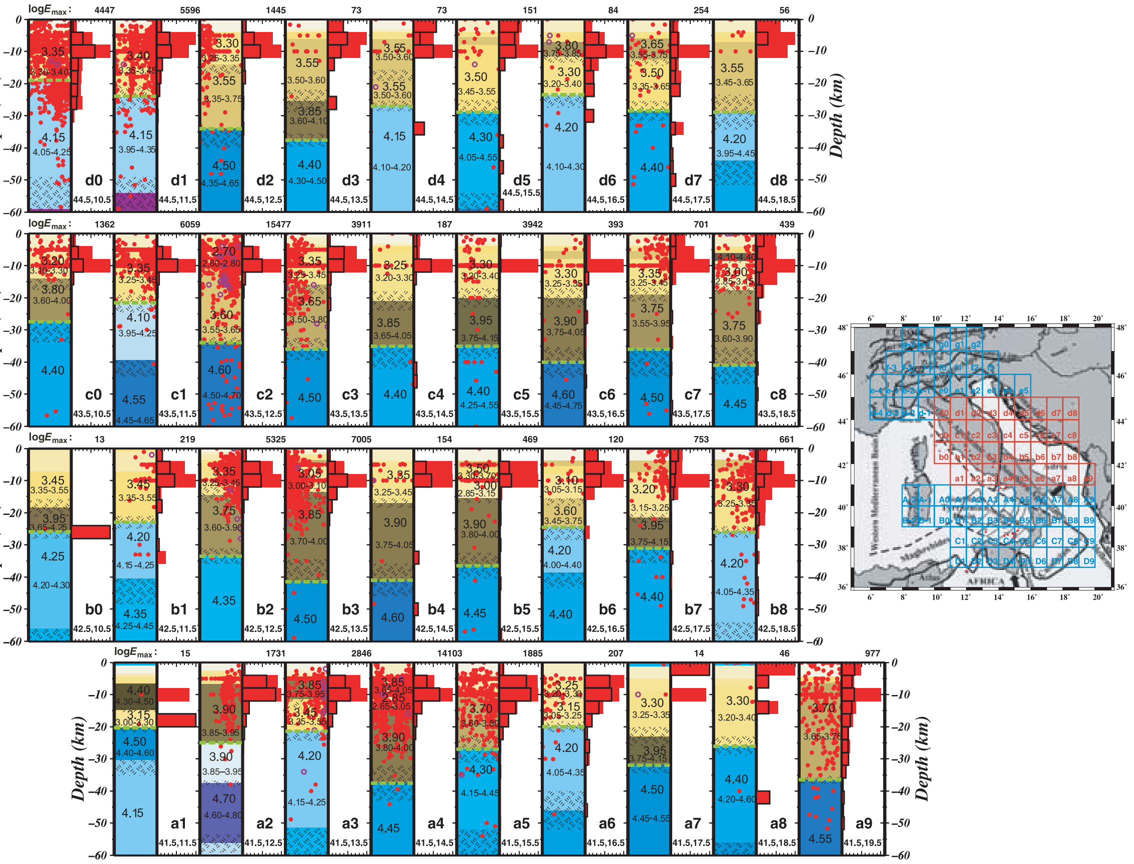

Fig. 2 The cellular *V*s structures and related log*E*–*h* distribution of seismicity in Central Italy and surroundings. See Fig. 1 for more details.

energy distribution vs. depth (log*E*–*h*) is shown in Figs 1–3 in the right hand graph for each cell. The logarithm of the energy for the grouped hypocentres was normalized to the maximal value logE_{max} for each cell (written on the horizontal energy axis). In each cell we considered all earthquakes listed in the ISC catalogue with depth and magnitude specified (red bar histogram) and only the earthquakes for which the depth had not been fixed a priori (black line histogram).

Discussion

The log*E*–*h* distribution for most of the cells is concentrated at depths of 4–12 km (Figs 1–3), similar to the distribution of earthquake frequency reported by Meletti and Valensise (2004) and with the maximum slightly shallower than in the distribution of hypocentres in the continental crust shown by Ponomarev (2007). The energy histograms of all events (red bars) and for the events for which the depth has not been fixed a priori (black line bars) have a similar behaviour (with some obvious exceptions for the cells with weak seismicity). Consistent with a classic Coulomb/Byerlee (brittle/ductile) transition, where the rheology and mechanical properties of rocks follow the Sibson's law for the upper crust, and a power law creep in the lower crust, the earthquake energy is concentrated in the upper crust (4–12 km); only in a few cells in the transition of the central-western Alps (f-3, f-2, f-1), the eastern Alps-Dinarides (e4, e5, d5), and the Dinarides-Hellenides (a9, A9) the earthquake energy is concentrated in the uppermost 10 km of the crust, generally with a maximum in the surface layers. These are thrust zones where orogenic processes are in progress, with predominant compression (Scandone and Stucchi, 2000), as it is evident from the focal mechanisms (Meletti and Valensise, 2004; Guidarelli and Panza, 2006; Pondrelli *et al.*, 2006). The energy release in the crust is dominant for the uppermost 60 km even in the zones with intermediate and deep seismicity (c2, b8, a9, A5, A9, C9, D3, D4, D5).

The ambiguities in our structural model are reduced with the addition of the hypocentre information, mainly in defining the location of the Moho (Panza *et al.*, 2007a). The cell a2, under the Albani hills and the Tyrrhenian offshore, is a clear example, where the definition of Moho is difficult using *V*s alone (Fig. 2). In this cell and in most of the southern Tyrrhenian Sea *V*s values usually observed in the crust (≤4.0 km s^{-1}) are interpreted as mantle material (Panza *et al.*, 2003,

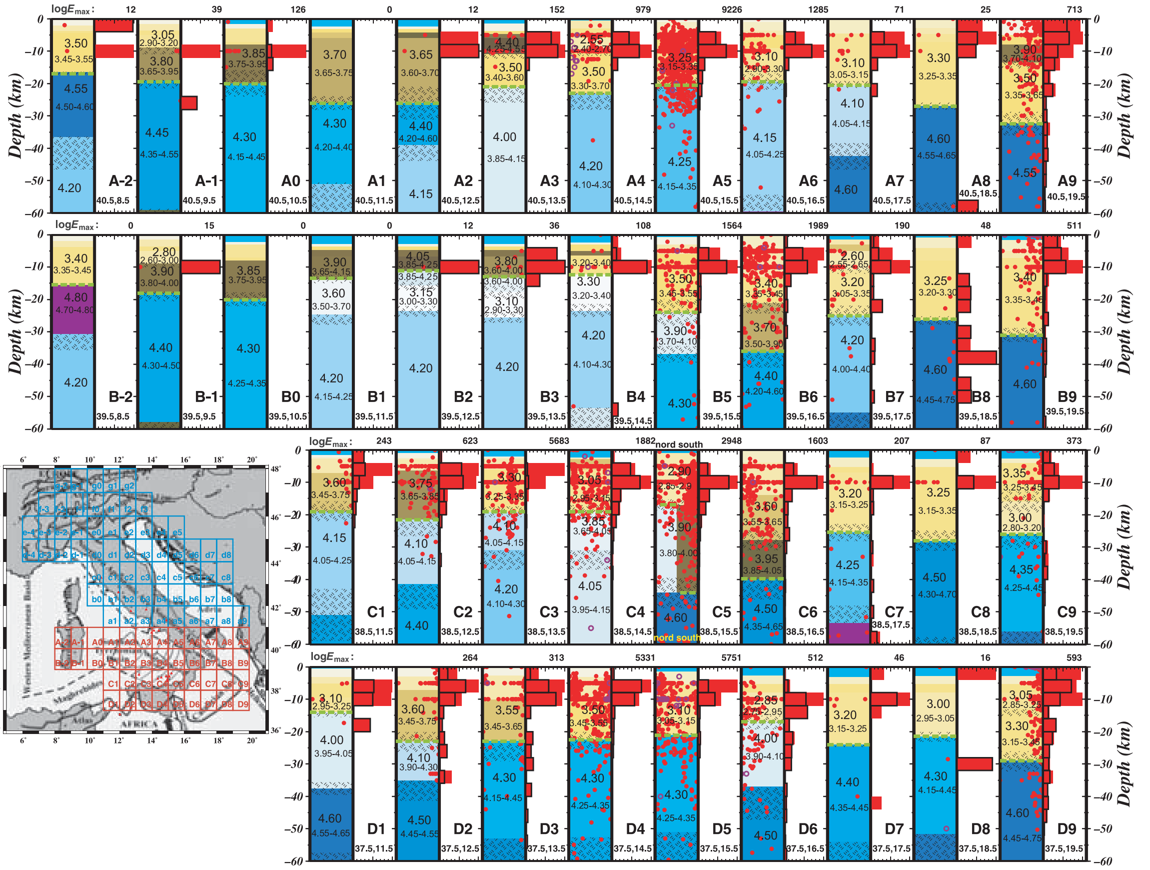

Fig. 3 The cellular Vs structures and related log$E$–h distribution of seismicity in Southern Italy and surroundings. The particular case of cell C5 is discussed in the text.

2007a,b), with a relatively high percentage of partial melting (Bottinga and Steinmetz, 1979; Green and Falloon, 2005). The upper crust in a2 reaches a depth of about 7 km with Vs about 3.3 km s^{-1}, and it overlies a 30-km-thick layer with Vs about 3.9 km s^{-1}. This layer is on top of a 20-km-thick high-velocity lid. According to the log$E$–h distribution and other data compilations (e.g. Nicolich and Dal Piaz, 1990) the 30-km-thick layer, with Vs about 3.9 km s^{-1}, can be reasonably assigned to the crust only up to a depth of about 25 km, where the recorded seismicity stops. The shut-down of the distribution of seismicity at a depth of about 25 km (Fig. 2) leaves room for an aseismic, ~12-km-thick, mantle layer. Therefore, the 3.9 km s^{-1} layer can be interpreted as high-velocity lower crust down to a depth of about 25 km, above a very low-velocity, soft mantle. The neighbouring cell a3 (Fig. 2) exhibits a negative velocity gradient within its 20-km-thick crust that overlies a low-velocity uppermost mantle layer with a Vs of about 4.2 km s^{-1} and a thickness of about 30 km. Below this layer, Vs increases with depth to an average of 4.35 km s^{-1}.

In e4 (Fig. 1) below about 23 km of depth, the 30-km-thick layer with Vs ~4.0 km s^{-1} can be lower crust (Moho boundary at ~53 km depth) or soft mantle (Moho boundary at ~23 km depth). The Moho depth defined by other studies varies between 35 and 45 km (Nicolich and Dal Piaz, 1990; Marone *et al.*, 2004; Dezes and Ziegler, 2005). The question can be settled considering the seismic energy distribution (Fig. 1) that is concentrated in the uppermost 30 km with some weak events below this depth: it is reasonable to assign the first 7 km of the 30-km-thick layer to the brittle continental crust, placing the Moho depth at about 30 km, and to interpret the remaining 23 km as very soft mantle.

The interpretation of Vs models in the cells with recent volcanism (b1, b2, a2, a3, A-2, A-1, A3, A4, A5, B-2, B-1, B1, B2, B4, C3, C4, C5, D2, D5) is given by Panza *et al.* (2007a). The seismicity, even if weak, in B2, B3, and B4 (Fig. 3) plays a key role in the definition of the Moho that can be placed just below the deepest event in each cell, namely, at depths of 11 km (B2), 13 km (B3), and 12 km (B4). In B2, the remaining 5 km, with Vs ~4.05 km s^{-1}, represent mantle material, cooler than the underlying very hot 8-km-thick mantle layer with average velocity 3.15 km s^{-1} and density 3.1 g cm^{-3}, followed by a layer with velocity 4.2 km s^{-1}. Similarly, in B3 the remaining 5 km of the layer with velocity 3.6–4.0 km s^{-1} is mantle material cooler than the underlying, very hot, 8-km-thick mantle with average velocity 3.1 km s^{-1} and density of 3.1 g cm^{-3}, followed by a layer with velocity 4.2 km s^{-1}. In B4, the hypocentre's distribution and gravity modelling define the remaining 11.5-km-thick layer with velocity 3.3 km s^{-1} and density 3.15 g cm^{-3} as mantle, followed by a layer with average velocity 4.2 km s^{-1}. There is no seismicity in B1 but, by analogy with the neighbouring cell B2 and with the results of gravity modelling, the layer with average velocity 3.6 km s^{-1} is defined as mantle with density 3.1 g m^{-3}. It overlies a layer with velocity 4.2 km s^{-1}.

Another interesting case is observed in the area of Stromboli and Messina strait to Southern Calabria, in C5 (Fig. 3). The nature of the crust is difficult to define as a layer with *V*s in the range 3.8–4.0 km s^{-1} reaching a depth of about 44 km overlies high-velocity mantle material. The analysis of the seismic energy distribution (details given in Panza *et al*., 2007a) leads to two distinct interpretations for this two-faced (Janus) crust/mantle layer. If we consider only the hypocentres at sea, this layer is totally aseismic and therefore it can be reasonably assigned to the mantle, consequently the crust has an average thickness of ~17 km. On the other hand, if all events in C5 are considered, the 'Janus' layer is occupied only by hypocentres located either in Sicily and Calabria (continental area) or close to their shoreline (Panza *et al*., 2007a). In such a case the layer can be reasonably assigned to the brittle continental crust which turns out to be ~40 km thick.

Finally, in d0, c1 (Fig. 2), D1, D2 and D6 (Fig. 3), seismic activity is recorded also in the uppermost mantle layer, where *V*s is relatively low, but where the average heat flow does not exceed 65 mW m^{-2} (95 mW m^{-2} for c1) according to Hurting *et al*. (1991). Gravity modelling in this region confirms that these layers belong to the mantle. The brittle behaviour of this uppermost mantle material, with average velocities 4.0–4.3 km s^{-1}, can be an example of the magma-assisted rifting model discussed by Buck (2004) and the eclogite mantle 'engine' by Anderson (2006).

From the integrated use of geophysical, petrological and geochemical data it is possible to confirm the presence of three processes that probably govern the present lithosphere dynamic in the Italian Peninsula and surroundings: delamination in North and Central Apennines (e.g. d0, d1, c1, b0, b1, a3) with mantle wedges that fill in the space left by the removed lithosphere along the W-directed subduction zones (Doglioni, 1991; Chimera *et al*., 2003; Panza *et al*., 2007b); slab detachments (e.g. A5, A6, B7), with low crust delamination and formation of orthopyroxene-rich uppermost mantle layer with strong crustal signatures (Lustrino, 2005), to continuous subduction in the Southern Apennines; slab roll-back and tearing with sideways asthenospheric flow through slab-windows in the Calabrian Arc (Panza *et al*., 2007a) with likely slab-detachment (e.g. C4, C5, D5, D6).

Conclusions

The synoptic representation of *V*s models of the uppermost 60 km of the Earth and of the log*E*–*h* distribution is used to define the Moho when its identification based on *V*s alone is ambiguous. For most of the cells, the earthquake energy released is maximum in the depth range of 4–12 km, i.e. mainly in the upper crust. For some regions where orogenic processes are in progress, the release of seismic energy is concentrated in the uppermost 10 km of the crust. The brittle behaviour of the uppermost mantle, with relatively low average velocities accompanied by relatively low heat flow, is well consistent with the magma-assisted rifting model and the eclogite mantle 'engine'.

Acknowledgements

The authors thank Luminita Ardeleanu, Gillian Foulger and Don Anderson for their very constructive comments and suggestions. Thanks to them the article, originated by a suggestion of Carlo Doglioni to publish the synoptic view of cellular models and seismicity contained in a DST internal database, has been significantly improved. Financial support has been given by ICTP Associates Scheme (R. Raykova), Italian Programma Nazionale di Ricerche in Antartide (PNRA) project 2004/2.7-2.8, Protezione Civile Regionale of Regione Friuli Venezia Giulia, and ASI Agenzia Spaziale Italiana (Italian Space Agency). This is a contribution to project S1 of Convenzione DPC-INGV 2007–09.

References

Anderson, D., 2006. The eclogite engine: chemical geodynamics as a Galileo thermometer. In: *The Origins of Melting Anomalies: Plates, Plumes, and Planetary Processes* (G.R. Foulger and D.M. Jurdy, eds). GSA book (in preparation), Available at: http://www.MantlePlumes.org (accessed on 07.03.2008).

Anderson, D., 2007. *Is there Convincing Tomographic Evidence for Whole Mantle Convection?* Available at: http://www.MantlePlumes.org (accessed on 07.03.2008).

Bottinga, Y. and Steinmetz, L., 1979. A geophysical, geochemical, petrological model of the sub-marine lithosphere. *Tectonophysics*, **55**, 311–347.

Boyadzhiev, G., Brandmayr, E., Pinat, T. and Panza, G.F., 2008. Optimization for nonlinear inverse problem. *Rendiconti Lincei: Scienze Fisiche e Naturali*, **19**, 17–43.

Buck, R., 2004. Consequences of asthenospheric variability on continental rifting. In: *Rheology and Deformation of the Lithosphere at Continental Margins* (G.D. Karner, B. Taylor, N.W. Driscoll and D.L. Kohlstedt, eds), 408 pp. Columbia University Press, Columbia, SC.

Cadoux, A., Blichert-Toft, J., Pinti, D.L. and Albarède, F., 2007. A unique lower mantle source for Southern Italy volcanics. *Earth Planet. Sci. Lett*., **259**, 227–238.

Carminati, E., Doglioni, C., Argnani, A., Carrara, G., Dabovski, C., Dumurdzanov, N., Gaetani, M., Georgiev, G., Mauffret, A., Nazai, S., Sartori, R., Scionti, V., Scrocca, D., Séranne, M., Torelli, L. and Zagorchev, I., 2004. TRANSMED transect III. In: *The TRANSMED Atlas — the Mediterranean Region from Crust to Mantle* (W. Cavazza, F. Roure, W. Spakman, G.M. Stampfli and P.A. Ziegler, eds), 141 pp. Springer-Verlag, Berlin.

Chimera, G., Aoudia, A., Saraò, A. and Panza, G.F., 2003. Active tectonics in central Italy: constraints from surface wave tomography and source moment tensor inversion. *Phys. Earth Planet. Int*., **138**, 241–261.

Dezes, P. and Ziegler, P., 2005. *Map of the European Moho*. EUCOR-URGENT: Available at: http://comp1.geol.unibas.ch/downloads/Moho_net/euromoho1_3.pdf (accessed on 07.03.2008).

Doglioni, C., 1991. A proposal of kinematic modelling for W-dipping subductions – possible applications to the Tyrrhenian-Apennines system. *Terra Nova*, **3**, 423–434.

Doglioni, C., Gueguen, E., Harabaglia, P. and Mongelli, F., 1999a. On the origin of W-directed subduction zones and applications to the western Mediterranean. *Geol. Soc. Sp. Publ.*, **156**, 541–561.

Doglioni, C., Harabaglia, P., Merlini, S., Mongelli, F., Peccerillo, A. and Piromallo, C., 1999b. Orogens and slabs vs their direction of subduction. *Earth Sci. Rev.*, **45**, 167–208.

Farina, B., 2006. *Lithosphere-asthenosphere system in Italy and surrounding areas: optimized non-linear inversion of surface-wave dispersion curves and modelling of gravity Bouguer anomalies*. Unpubl. doctoral disertation. DST, University of Trieste, Trieste, 278 pp.

Gasperini, P., 2002. Local magnitude revaluation for recent Italian earthquakes (1981–1996). *J. Seismol.*, **6**, 503–524.

Green, D.H. and Falloon, T.J., 2005. Primary magmas at mid-ocean ridges, "hotspots", and other intraplate settings: Constraints on mantle potential temperature. Special Paper 388, *Plates, plumes and paradigma*, **388**, 217–247.

Guidarelli, M. and Panza, G.F., 2006. INPAR, CMT and RCMT seismic moment solutions compared for the strongest damaging events ($M^3 4.8$) occurred in the Italian region in the last decade. *Rend. Accad. Naz. Sci. XL Mem. Sci. Fis. Natur.*, **30**, 81–98.

Herak, M., Panza, G.F. and Costa, G., 2001. Theoretical and observed depth correction for Ms. *Pure Appl. Geophys.*, **158**, 1517–1530.

Hoernle, K., Zhang, Yu.-S. and Graham, D., 1995. Seismic and geochemical evidence for large-scale mantle upwelling beneath the eastern Atlantic and western and central Europe. *Nature*, **374**, 34–39.

Hurting, E., Cermak, V., Haenel, R. and Zui, V. (eds), 1991. *Geothermal Atlas of Europe*. Hermann Haack Verlag, Gotha, 156 pp.

ISC, 2007. *On-line Bulletin*. International Seismological Centre, Bergshire, UK. Available at: http://www.isc.ac.uk (accessed on 07.03.2008).

Lustrino, M., 2005. How the delamination and detachment of lower crust can influence basaltic magmatism. *Earth Sci. Rev.*, **72**, 21–38.

Marone, F., van der Lee, S. and Giardini, D., 2004. Three-dimensional upper-mantle S-velocity model for the Easia-Africa plate boundary region. *Geophys. J. Int.*, **158**, 109–130.

Meletti, C. and Valensise, G., 2004. Zonazione sismogenetica ZS9 – App. 2 al Rapporto Conclusivo. In: *Gruppo di Lavoro MPS (2004). Redazione della mappa di pericolosità sismica prevista dall'*Ordinanza PCM 3274 del 20 marzo 2003. Rapporto Conclusivo per il Dipartimento della Protezione Civile, INGV, Milano-Roma, Aprile 2004, 65 pp. + 5 Allegati.

Meletti, C., Patacca, E. and Scandone, P., 2000. Construction of a seismotectonic model: the case of Italy. *Pure Appl. Geophys.*, **157**, 11–35.

Nicolich, R. and Dal Piaz, R., 1990. Moho isobaths. In: *Structural Model of Italy and Gravity Map* (G. Bigi, D. Cosentino, M. Parotto, R. Sartori and P. Scandone, ed). *Quad. Ric. Sci.*, **114**, 3.

Panza, G.F., 1981. The resolving power of seismic surface waves with respect to crust and upper mantle structural models. In: *The Solution of the Inverse Problem in Geophysical Interpretation* (R. Cassinis, ed.), pp. 39–77. Plenum Press, New York.

Panza, G.F and Pontevivo, A., 2004. The Calabrian Arc: a detailed structural model of the lithosphere-asthenosphere system. *Rend. Accad. Naz. Sci. XL Mem. Sci. Fis. Natur.*, **28**, 51–88.

Panza, G.F., Pontevivo, A., Chimera, G., Raykova, R.B. and Aoudia, A., 2003. The lithosphere-asthenosphere: Italy and surroundings. *Episodes*, **26**, 169–174.

Panza, G.F., Peccerillo, A., Aoudia, K. and Farina, B., 2007a. Geophysical and petrological modelling of the structure and composition of the crust and upper mantle in complex geodynamic settings: the Tyrrhenian sea and surroundings. *Earth Sci. Rev.*, **80**, 1–46.

Panza, G.F., Raykova, R., Carminati, E. and Doglioni, C., 2007b. Upper mantle flow in the western Mediterranean. *Earth Planet. Sci. Lett.*, **257**, 200–214.

Peccerillo, A., 2005. *Plio-Quaternary Volcanism in Italy. Petrology, Geochemistry, Geodynamics*. Springer, Heidelberg, 365 pp.

Peishan, C. and Haitong, C., 1989. Scaling law and its applications to earthquake statistical relations. *Tectonophysics*, **188**, 53–72.

Pondrelli, S., Salimbeni, S., Ekström, G., Morelli, A., Gasperini, P. and Vannucci, G., 2006. The Italian CMT dataset from 1977 to the present. *Phys. Earth Planet. Inter.*, **159**, 286–303.

Ponomarev, V.S., 2007. Denudation and Seismicity of the Earth's Crust. *Doklady Earth Sci.*, **412**, 19–21.

Richter, C.F., 1958. *Elementary Seismology*. W. H. Freeman & Co., San Francisco.

Scandone, P. and Stucchi, M., 2000. La sonazione sismogenetica ZS4 come strumento per la valutazione della pericolositàsismica. In: *Le Ricerche del GNDT nel Campo della Pericolozità Sismica (1996-1999)* (F. Galadini, C. Meletti, A. Rebez, eds), pp. 3–14. Gruppo Nazionale per la difesa dai Terremoti, Roma.

Yanovskaya, T.B., 1997. Resolution estimation in the problems of seismic ray tomography. *Izv. Phys. Solid Earth*, **33**, 762–765.

Yanovskaya, T.B. and Ditmar, P.G., 1990. Smoothness criteria in surfacewave tomography. *Geophys. J. Int.*, **102**, 63–72.

Received 28 November 2007; revised version accepted 17 February 2008

